

# A Theoretical View on $\text{Co}^+$ -Mediated C–C and C–H Bond Activations in Ethane

Max C. Holthausen<sup>†</sup> and Wolfram Koch\*

Contribution from the Institut für Organische Chemie der Technischen Universität Berlin, Strasse des 17. Juni 135, D-10623 Berlin, Germany

Received December 5, 1995<sup>⊗</sup>

**Abstract:** The potential energy surface corresponding to the reaction of the cobalt cation with ethane, which represents a prototype of the activation of C–C and C–H bonds in alkanes by transition metal cations, has been investigated by employing the recently suggested density functional theory/Hartree–Fock hybrid method B3LYP combined with reasonably large one-particle basis sets. The quality of this approach has been calibrated against experimentally known  $\text{Co–R}^+$  binding energies of possible exit channels and against CCSD(T) energy calculations. The performance of the chosen model is satisfying with respect to the description of relative energies, although some nonuniform deviations between calculated and experimental data have been found for absolute binding energies. The calculated barriers for the initial insertion steps of  $\text{Co}^+$  into C–C and C–H bonds are undoubtedly found to be considerably less energy demanding than the activation barriers connected with the reductive elimination of  $\text{H}_2$  and  $\text{CH}_4$ , respectively. The rate determining step for the C–C activation branch is a 1,3-H shift leading to a complex between  $\text{Co}(\text{CH}_2)^+$  and methane. Along the C–H activation reaction coordinate, a concerted saddle point connecting the C–H inserted species directly with a complex of  $\text{Co}^+$  with molecular hydrogen and ethylene has been identified as the energetic bottleneck. Despite of being often proposed, no inserted dihydrido species could be located.

## Introduction

The C–H and C–C bond activations of alkanes brought about by bare transition metal ions are of fundamental interest in various areas of chemical research, such as organic chemistry, biochemistry, and, probably most important,<sup>1</sup> catalytic research. The oxidative addition and reductive elimination of ligands are two of the most fundamental steps in reactions occurring at metal centers in catalytic processes. A rigorous understanding of elementary processes taking place at reactive centers is a prerequisite for the development of working hypotheses for synthetic chemistry. From an experimental point of view, mass spectrometric studies of gas phase reactions between transition metal ions and organic substrates are a powerful tool to assess intrinsic binding properties and the reactivity of these species without the cooperative influences of further ligands, counterions, or solvent molecules.<sup>2</sup> Such techniques have provided a wealth of accurate thermochemical data, such as  $\text{M}^+–\text{R}$  binding energies, for a wide variety of organometallic compounds. In spite of this impressive progress, a complete characterization of the actual reaction mechanisms, i.e. explicit information on the structural and energetical details of all intermediates and transition structures involved in the course of a particular reaction, is, however, possible only in lucky cases by experimental means alone. Quantum chemical calculations in principle offer a complementary source of information. However, even if only qualitative accuracy in the field of open-shell transition metal compounds is desired in the framework of conventional ab initio molecular orbital theory, a sophisticated treatment of both near-degeneracy as well as dynamic electron

correlation effects is required, and the application of such methods is usually restricted to rather small molecules. As a promising alternative, which combines reasonable accuracy with computational efficiency, density functional theory (DFT) and in particular DFT/Hartree–Fock hybrid methods have recently attracted considerable attention. These methods have been successfully applied by us and others to study various open-shell transition metal compounds.<sup>3</sup> In a very recent investigation, we employed the DFT/HF approach for the first time to a complete reaction sequence involving open-shell transition metal species: the reactions of  $\text{Fe}^+$  and ethane, one of the prototype systems for transition metal cation mediated C–H and C–C bond activations in alkanes.<sup>4</sup> In the present contribution we present a comprehensive quantum chemical picture of the reaction of cationic cobalt with ethane. We apply the DFT/HF approach to characterize all minima and saddle points on the  $[\text{Co}, \text{C}_2, \text{H}_6]^+$  potential energy surface (PES) relevant for the C–H and C–C bond activations and present a complete mechanistic scenario for this important reaction sequence. The results will be analyzed in light of the available experimental and theoretical information.

## Computational Strategy

The computational approach employed in the present study closely follows our earlier work and has been described in detail in these publications.<sup>3a,b,4</sup> We use the “Becke-3-LYP” func-

<sup>†</sup> Present address: Cherry L. Emerson Center for Scientific Computations and Department of Chemistry, Emory University, Atlanta, GA 30322.

\* E-mail: kochw@argon.chem.tu-berlin.de.

<sup>⊗</sup> Abstract published in *Advance ACS Abstracts*, October 1, 1996.

(1) Haggin, J. *Chem. Eng. News* **1993**, 71 (May 31), 27.

(2) For recent reviews see: (a) Schröder, D.; Schwarz, H. *Angew. Chem.* **1995**, 107, 2126; *Angew. Chem., Int. Ed. Engl.* **1995**, 34, 1973. (b) Eller, K.; Schwarz, H. *Chem. Rev.* **1991**, 91, 1121. (c) Freiser, B. S. *Acc. Chem. Res.* **1994**, 27, 353.

(3) See, e.g.: (a) Holthausen, M. C.; Heinemann, C.; Cornehl, H. H.; Koch, W.; Schwarz, H. *J. Chem. Phys.* **1995**, 102, 4931. (b) Holthausen, M. C.; Mohr, M.; Koch, W. *Chem. Phys. Lett.* **1995**, 240, 245. (c) Heinemann, C.; Schwarz, H.; Koch, W.; Dyll, K. G. *J. Chem. Phys.* **1996**, 104, 4642. (d) Ricca, A.; Bauschlicher, C. W., Jr. *Chem. Phys. Lett.* **1995**, 245, 150. (e) Ricca, A.; Bauschlicher, C. W., Jr. *Theor. Chim. Acta* **1995**, 92, 123. (f) Ricca, A.; Bauschlicher, C. W., Jr. *J. Phys. Chem.* **1995**, 99, 5922. (g) Barone, V. *Chem. Phys. Lett.* **1995**, 233, 129. (h) Barone, V. *J. Phys. Chem.* **1995**, 99, 11659. (i) Adamo, C.; Lelj, F. *Chem. Phys. Lett.* **1995**, 246, 463. (j) Barone, V.; Adamo, C. *J. Phys. Chem.* **1996**, 100, 2094.

(4) (a) Holthausen, M. C.; Fiedler, A.; Schwarz, H.; Koch, W. *Angew. Chem.* **1995**, 107, 2430; *Angew. Chem., Int. Ed. Engl.* **1995**, 34, 2282. (b) *J. Phys. Chem.* **1996**, 100, 6236.

tional<sup>5</sup> (abbreviated as B3LYP) as implemented in the DFT module of Gaussian92/DFT.<sup>6</sup> This functional was combined with the standard D95\*\* polarized double- $\zeta$  basis set<sup>7</sup> for carbon and hydrogen. For cobalt the (14s9p5d) primitive set of Wachters<sup>8</sup> supplemented with one diffuse p-function ( $\alpha = 0.1219$ ) and one diffuse d-function according to Hay<sup>9</sup> is used, resulting in a (6211111|33121|411)  $\rightarrow$  [8s5p3d] contraction. We calculated the  $\text{Co}^+(\text{3F})/\text{Co}^+(\text{5F})$  atomic state splitting by employing integer electron occupation numbers of orbitals in the Mulliken population analysis, which are chosen according to Hay.<sup>9</sup> Stationary points were localized using analytical gradients and their character (minimum, transition structure, or higher order saddle point) was determined from the analytically computed force constant matrices. As for the  $[\text{Fe}, \text{C}_2\text{H}_6]^+$  PES, we encountered some cases, where the determination of a converged optimized structure required the analytically determined Hessian matrix and/or a slightly breaking of the molecular point group symmetry. All structures discussed in the text correspond to fully optimized geometries with both the gradients as well as the displacements from analytical second derivatives below the standard convergence criteria. Spin contamination of the unrestricted B3LYP open-shell determinants was in all cases very small, the deviation of the  $\langle S^2 \rangle$  expectation values for the open-shell species never exceeded 5%.<sup>10</sup> In order to allow for a more direct comparison to experiment, we corrected our calculated energies to 0 K by including zero-point vibrational energy (ZPVE) contributions. Due to the known problems<sup>11</sup> of rotational invariance in the grid integration technique in Gaussian92/DFT the frequency calculations of some structures showed non-zero rotational frequencies. Since deviations in the lowest frequencies contribute directly to the calculation of thermodynamic properties, we do not correct our results for thermal contributions, which are expected to be small anyway.

CCSD(T)<sup>12</sup> energy calculations were performed in order to gauge the B3LYP method on the stationary points and the entrance and exit channels on the PES by means of the Gaussian92/DFT package. The optimized geometries and ZPVE from the corresponding B3LYP computations have been used. The same basis set as for the B3LYP calculations has been employed, augmented with a singly contracted f-polarization function for the Co atom based on a three-term fit to a Slater-type orbital<sup>13</sup> resulting in a contraction [8s5p3d1f]. This one particle basis set is a remnant of several benchmark computations and must certainly be viewed as a “minimal” basis set for the application of coupled cluster methods to open-shell transition metals. However, we were urged to this level by the

(5) (a) Becke, A. D. *J. Chem. Phys.* **1993**, *98*, 5648. *Ibid.* **1993**, *98*, 1372. (b) Stephens, P. J.; Devlin, F. J.; Chabalowski, C. F.; Frisch, M. J. *J. Phys. Chem.* **1994**, *98*, 11623.

(6) GAUSSIAN92/DFT Rev. F.2: Frisch, M. J.; Trucks, G. W.; Schlegel, H. W.; Gill, P. M. W.; Johnson, B. G.; Wong, M. W.; Foresman, J. B.; Robb, M. A.; Head-Gordon, M.; Replogle, E. S.; Gomperts, R.; Andres, J. L.; Raghavachari, K.; Binkley, J. S.; Gonzales, C.; Martin, R. L.; Fox, D. J.; DeFrees, D. J.; Baker, J.; Stewart, J. J. P.; Pople, J. A.; GAUSSIAN Inc.: Pittsburgh, PA, 1992.

(7) Dunning, T. H.; Hay, P. J. In *Modern Theoretical Chemistry*; Schaefer, H. F., III, Ed.; Plenum Press: New York, 1977; Vol. II.

(8) Wachters, A. J. H. *J. Chem. Phys.* **52**, 1033.

(9) Hay, P. J. *J. Chem. Phys.* **1977**, *66*, 4377.

(10) It is well-known that spin contamination is less problematic in unrestricted Kohn–Sham determinants: Baker, J.; Scheiner, A.; Andzelm, J. *J. Chem. Phys. Lett.* **1993**, *216*, 380.

(11) Johnson, B. G.; Frisch, M.; *J. Chem. Phys. Lett.* **1993**, *216*, 133. Johnson, B. G.; Gill, P. M. W.; Pople, J. A. *J. Chem. Phys. Lett.* **1994**, *220*, 377. Johnson, B. G. In *Modern Density Functional Theory: A Tool for Chemistry*; Seminario, J. M.; Politzer, P., Eds.; Elsevier: New York, 1995.

(12) For recent reviews, see: Bartlett, R. J. In *Reviews in Computational Chemistry*; Lipkowitz, K. B.; Boyd, D. B., Eds.; VCH: New York, 1994; Vol. 5. Bartlett, R. J. In *Modern Electronic Structure Theory*; Yarkony, D. R., Ed.; World Scientific: Singapore, 1995; Part II.

(13) Stewart, R. F. *J. Chem. Phys.* **1970**, *52*, 431.

**Table 1.** Calculated and Experimental Binding Energies (kcal mol<sup>-1</sup>)

species	d-pop. <sup>a</sup>	$D_e$	$D_0$	$D_{0,\text{corr}}^b$	exptl	previous comp	$D_0$
$\text{Co}^+=\text{CH}_2$	7.62	79	76	78	78 <sup>c</sup>	70, <sup>e</sup> 80 <sup>f</sup>	
$\text{CO}^+-\text{H}$	7.38	46	44	47	46 <sup>c</sup>	41, <sup>g</sup> 44, <sup>h</sup> 48 <sup>i</sup>	
$\text{CO}^+-\text{CH}_3$	7.43	49	46	49	48 <sup>c</sup>	43 <sup>j</sup>	
$\text{CO}^+-\text{C}_2\text{H}_5$	7.50	56	54	57	47 <sup>c</sup>		
$\text{Co}(\text{CH}_4)^+$	7.97	24	24	24	22, <sup>c</sup> 23 <sup>d</sup>	20, <sup>f</sup> 21 <sup>k</sup>	
$\text{Co}(\text{C}_2\text{H}_6)^+$	7.99	29	29	29	24, <sup>c</sup> 28 <sup>d</sup>	24 <sup>k</sup>	
$\text{Co}(\text{H}_2)^+$	7.97	20	19	19	18 <sup>c,d</sup>	16, <sup>k</sup> 15, <sup>l</sup> 19 <sup>m</sup>	
$\text{Co}(\text{H}_2)^+$	7.97	20	19	19	18 <sup>c,d</sup>	16, <sup>k</sup> 15, <sup>l</sup> 19 <sup>m</sup>	
$\text{Co}(\text{C}_2\text{H}_4)^+$	7.83	51	50	51	43 <sup>c</sup>	36 <sup>n</sup>	
species	$D_e$	$D_0$	exptl <sup>o</sup>	species	$D_e$	$D_0$	exptl <sup>o</sup>
H–H	113	106	104	$\text{CH}_3-\text{CH}_3$	92	83	90
$\text{CH}_3-\text{H}$	113	104	105	$\text{H}_2\text{C}=\text{CH}_2$	175	165	174
				$\text{C}_2\text{H}_5-\text{H}$	108	99	100

<sup>a</sup> B3LYP occupation of  $\text{Co}^+(3d)$  orbitals according to the NBO analysis. <sup>b</sup> “corr-B3LYP” results obtained according to ref 3d. <sup>c</sup> Reference 17. <sup>d</sup> Reference 18. <sup>e</sup> Reference 48. <sup>f</sup> Reference 32. <sup>g</sup> Reference 49. <sup>h</sup> Reference 50. <sup>i</sup> Reference 51. <sup>j</sup> Reference 52. <sup>k</sup> Reference 23. <sup>l</sup> Reference 53. <sup>m</sup> Reference 54. <sup>n</sup> Reference 55. <sup>o</sup> Reference 56.

extreme computational demands of the CCSD(T) method applied to the systems under study. On the other hand, similar sized basis sets have been shown to yield reasonably accurate results, at least in a qualitative sense.<sup>14</sup>

## Results and Discussion

In the following we will first establish the accuracy that can be expected from the B3LYP approach for the molecules under investigation. Then, we will present our results for the C–C and C–H bond activation branches of the  $[\text{Co}, \text{C}_2\text{H}_6]^+$  PES and compare them to our earlier conclusions drawn for the related  $[\text{Fe}, \text{C}_2\text{H}_6]^+$  system.<sup>4</sup> Finally, the implications of the present work for gas phase experiments will be discussed in light of the most recent experimental and theoretical data available.

**Calibration.** In our work on the  $[\text{Fe}, \text{C}_2\text{H}_6]^+$  PES, we showed<sup>4</sup> that the B3LYP ansatz tends to overestimate  $\text{Fe}^+-\text{R}$  (where R represents an organic fragment) binding energies by up to 18 kcal mol<sup>-1</sup> while the relative stabilities of various exit channels with respect to the  $\text{Fe}^+(\text{6D}) + \text{C}_2\text{H}_6$  asymptote were reproduced with much smaller errors, the largest being 4 kcal mol<sup>-1</sup>. We attributed the disappointing quantitative performance of the DFT/HF method for the calculation of  $\text{Fe}^+-\text{R}$  binding energies in part to the well-known bias of DFT toward  $3d^n$  over  $4s^1 3d^{n-1}$  configurations.<sup>3a,b,d,15</sup> In the case of iron, this leads to an incorrect ordering of the atomic states, where B3LYP erroneously predicts the  $^4\text{F}$  ( $3d^7$ ) state to be more stable than the experimental  $^6\text{D}$  ( $4s^1 3d^6$ ) ground state (calcd,  $-2.8$ ; expt,<sup>16</sup> 5.8 kcal mol<sup>-1</sup>). For  $\text{Co}^+$  with its  $3d^8$  ground state configuration the situation is similar: B3LYP gives the correct ordering of atomic states, but due to the bias toward  $3d^n$  over  $4s^1 3d^{n-1}$  configurations, the excitation energy to the  $^5\text{F}$  ( $4s^1 3d^7$ ) state is overestimated by 5.2 kcal mol<sup>-1</sup> (calcd, 15.1; expt,<sup>16</sup> 9.9 kcal mol<sup>-1</sup>). This is in agreement with a recent B3LYP study of Ricca and Bauschlicher, who calculated a splitting of 15.6 kcal mol<sup>-1</sup>, using a similar basis set.<sup>3d</sup> Table 1 collects the theoretically predicted binding energies corrected to 0 K in comparison with the most reliable experimental and previous computational data for a representative set of molecules that are of importance for a description of the  $\text{Co}^+ + \text{C}_2\text{H}_6$  interaction. Our  $D_0$  values show an average deviation from the

(14) Blomberg, M. R. A.; Siegbahn, P. E. M.; Lee, T. L.; Rendell, A. P.; Rice, J. E. *J. Chem. Phys.* **1991**, *95*, 5898.

(15) Ziegler, T.; Li, J. *Can. J. Chem.* **1994**, *72*, 783.

(16)  $j$ -averaged value calculated from the following: Moore, C. E. *Atomic Energy Level*. Natl. Bur. Stand. (U.S.), Circ. 467: Washington, DC, 1949.

**Table 2.** Experimental and Calculated Energies Relative to Separated  $\text{Co}^+(\text{}^3\text{F}) + \text{C}_2\text{H}_6$  (kcal mol<sup>-1</sup>)

exit channel	exptl <sup>a</sup>	B3LYP <sup>b</sup>
$\text{Co}^+ + \text{C}_2\text{H}_6$	0	0
$\text{CoCH}_3^+ + \text{CH}_3^*$	41	36
$\text{CoCH}_2^+ + \text{CH}_4$	19	14
$\text{Co}(\text{H}_2)^+ + \text{C}_2\text{H}_4$	15	14
$\text{Co}(\text{C}_2\text{H}_4)^+ + \text{H}_2$	-10	-17
$\text{CoH}^+ + \text{C}_2\text{H}_5^*$	54	56
$\text{CoC}_2\text{H}_5^+ + \text{H}^*$	53	45

<sup>a</sup> Experimental data taken from ref 56. <sup>b</sup> Calculated results include corrections for ZPVE contributions.

experimental values of 3.4 kcal mol<sup>-1</sup> with a maximum deviation of 7 kcal mol<sup>-1</sup> (for  $\text{Co}^+-\text{C}_2\text{H}_5$ ), interestingly, the  $D_0$  values for  $\text{Co}^+-\text{H}$  and  $\text{Co}^+-\text{CH}_3$  are in error by only 2 kcal mol<sup>-1</sup> if based on the experimental data from ref 17. If the recent experimental results derived from equilibrium methods of Kemper et al.<sup>18</sup> are used for  $\text{Co}(\text{C}_2\text{H}_6)^+$  and  $\text{Co}(\text{CH}_4)^+$ , the agreement between theory and experiment is improved further to an average deviation of 2.6 kcal mol<sup>-1</sup> (the maximum deviation remains unchanged). It is also important to note that the B3LYP results have about the same quality as the previous theoretically determined binding energies, which were usually obtained by elaborate, highly correlated wave function based methods. As apparent from Table 1, the strength of the C–C bonds in ethane and ethylene are described slightly too weak whereas the calculated C–H binding energies are in good agreement with the experimental results. The results for the relative energies of the exit channels are shown in Table 2. The average error is 4.7 kcal mol<sup>-1</sup> with a maximum deviation of 8 kcal mol<sup>-1</sup>. Even though these results are quite satisfactory, a word of caution is required. It must be kept in mind that the error is not constant but subject to large variations, if different bonding situations are present. Errors in the calculations of the atomic state splitting of  $\text{Co}^+$  may have further implications for binding energies, since the bonding in all  $\text{Co}^+-\text{R}$  species considered is a mixture of the  $4s^13d^7$  and  $3d^8$  configurations on cobalt. But unlike for the conventional ab initio MO methods, where the source of error can usually be traced back to deficiencies in the description of the one or many particle problem and systematic procedures for reducing these errors exist, the reasons *why* in the DFT calculations some systems are better described than others are not fully understood yet and no systematic way of improving the results is known. In a recent publication<sup>3d</sup> Ricca and Bauschlicher proposed a correction scheme to B3LYP, very similar to a commonly used scheme in the world of conventional *post*-HF computations. Their “corr-B3LYP” results for binding energies of a set of molecular complexes  $\text{M}^+=\text{CH}_2$  ( $\text{M} = \text{Sc}-\text{Cu}$ ) have been obtained by computing the dissociation energy of a molecular complex with respect to both, the calculated atomic ground state asymptotes, in the case of  $\text{Co}^+ 3d^8$ , and the first excited state, here the  $4s^13d^7$  configuration, and using the experimental atomic separation to obtain the binding energy to the ground state asymptote. Then, they compute the weighted average of these two values according to the metal 3d population, which introduces a weighted correction for the erroneous atomic state splitting for molecular complexes. If we follow this idea and correct the  $D_0$  values for  $\text{Co}^+-\text{R}$  in Table 1, the average error is slightly increased from 3.4 to 3.9 kcal mol<sup>-1</sup>. Not only does the overall performance of this correction here<sup>19</sup> work in the wrong direction but also it does not account for the obvious

(17) Armentrout, P. B.; Kickel, B. L. In *Organometallic Ion Chemistry*; Freiser, B. S., Ed., submitted for publication.

(18) Kemper, P. R.; Bushnell, J. E.; van Koppen, P. A. M.; Bowers, M. T. *J. Phys. Chem.* **1993**, *97*, 1810.

different quality in the description of different binding situations, e.g. of  $\text{CoCH}_2^+$  and  $\text{Co}(\text{C}_2\text{H}_4)^+$  (cf. Table 1). Unfortunately, it is by no means clear to which extent the *underlying reason* of the error in the description of atomic state splittings carries over to the molecular environment. It has recently been shown<sup>20</sup> that in modern gradient corrected functionals errors are non-uniformly distributed over a molecular environment and that error compensation effects could be in part responsible for the good performance of nonlocal DFT computations. No such careful analysis is existent for the presently used HF/DFT hybrid functionals, and we feel that this precludes a simple and universal correction scheme for molecular complexes solely based on errors in atomic state splittings.

In summary, while one must not forget that the aforementioned shortcomings of the B3LYP approach to some extent limit the predictive power in *quantitative* terms, we are nonetheless confident that it correctly describes the *qualitative* features of the PES governing the mechanistic details of the C–H and C–C bond activation reactions.

**C–C Bond Activation.** We will begin by discussing the interaction of a cobalt cation with the carbon–carbon bond in ethane. All energies given in the following refer to  $D_0$  values. The geometries of all relevant minima and saddle points are depicted in Figure 1, while Figure 2 shows the C–C bond activation branch of the triplet  $[\text{Co}, \text{C}_2, \text{H}_6]^+$  PES.<sup>21</sup> The interaction of a  $\text{Co}^+(\text{}^3\text{F})$  ground state ion with ethane leads initially to the formation of a predominantly electrostatically bound  $\text{Co}(\text{C}_2\text{H}_6)^+$  adduct, **1**. This cobalt ion–ethane complex has  $C_2$  symmetry, similar to the geometry given by Rosi *et al.*<sup>22</sup> for the corresponding ethane complex with  $\text{Cu}^+$  but unlike the ethane complexes of  $\text{Cr}^+$ ,  $\text{Mo}^+$ , and  $\text{Fe}^+$ , which assume  $C_s$  symmetric geometries. In their recent ab initio MO investigation of molecular complexes of small alkanes with  $\text{Co}^+$ , Perry *et al.*<sup>23</sup> identified a  $C_s$  structure as the most stable  $\text{Co}(\text{C}_2\text{H}_6)^+$  complex; however, the  $C_2$  isomer was found to be energetically almost degenerate, lying only 0.1 kcal mol<sup>-1</sup> higher in energy. In our calculations, the  $C_s$  structure is 1 kcal mol<sup>-1</sup> above the  $C_2$  form and characterized as a saddle point by one imaginary frequency of 195i cm<sup>-1</sup>. Obviously, these energy differences are too small to allow for a definitive statement regarding the ground state geometry of the  $\text{Co}(\text{C}_2\text{H}_6)^+$  adduct. The cobalt hydrogen distance in **1** amounts to 1.871 Å, while the distance to the carbon atoms is computed to be 2.289 Å. For comparison, Perry *et al.*<sup>23</sup> determine these distances as 1.96 and 2.34 Å based on partial geometry optimizations. **1** is predicted to be more stable than the  $\text{Co}^+(\text{}^3\text{F}) + \text{C}_2\text{H}_6$  entrance channel by 29 kcal mol<sup>-1</sup>, slightly overestimating the experimental  $\text{Co}^+-\text{ethane}$  binding energy of 24 kcal mol<sup>-1</sup> given in ref 17. However, our result is in perfect agreement with recent experimental work of Kemper *et al.*, who derived a binding energy of  $28 \pm 1.6$  kcal mol<sup>-1</sup> for  $\text{Co}(\text{C}_2\text{H}_6)^+$  from equilibrium methods.<sup>18</sup> The adduct complex can rearrange to a second species, in which the cobalt has been inserted into the C–C bond, leading to the dimethyl species **2**. This ion is computed to be 15 kcal mol<sup>-1</sup>

(19) The application of this correction scheme for the carbene complexes of the first transition metal row in fact decreases the overall error of the binding energies.<sup>3d</sup> However, as in our study,  $D_0(\text{Co}^+=\text{CH}_2)$  is slightly deteriorated.

(20) van Leeuwen, R.; Baerends, E. J. *Int. J. Quantum Chem.* **1994**, *52*, 711.

(21) While the corresponding processes in the  $\text{Fe}^+$ /ethane system involved a sextet  $\rightarrow$  quartet spin flip in the initial stage of the reaction sequence,<sup>4</sup> no such conversion is necessary in the present system. All processes described here occur on the triplet surface.

(22) Rosi, M.; Bauschlicher, C. W., Jr.; Langhoff, S. R.; Partridge, H. J. *Phys. Chem.* **1990**, *94*, 8656.

(23) Perry, J. K.; Ohanessian, G.; Goddard, W. A., III. *J. Phys. Chem.* **1993**, *97*, 5238.

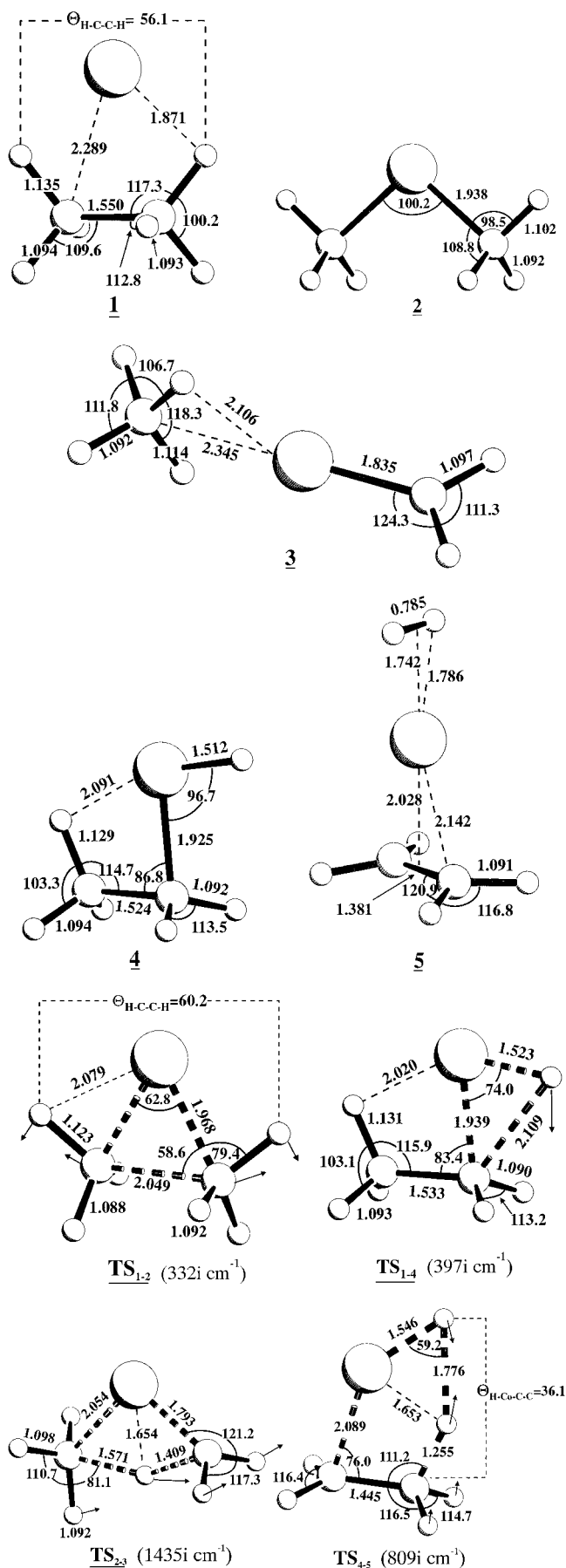


**Figure 1.** Optimized geometries. Bond lengths in Å; angles in degrees. For the transition states, the transition vectors, i.e., the normal modes corresponding to the imaginary frequencies, are also shown.

less stable than **1**. A comparison of the B3LYP optimized structure of **2** with the data from a partial geometry optimization at the MCPF level reported by Rosi *et al.*<sup>22</sup> shows good agreement between the two methods, e.g. the Co–C distance and C–Co–C angle are 1.938 Å and 100.2° at the B3LYP level and 1.985 Å and 101.2° at the MCPF level, respectively. In a recent high-level ab initio study on this ion, Perry *et al.* given similar values of 1.977 Å and 98.3° for the Co–C distance and the C–Co–C angle, respectively, obtained using CASSCF/MRCI wave functions.<sup>24</sup> The isomerization **1** → **2** is connected with an activation barrier of 21 kcal mol<sup>-1</sup> with respect to **1** proceeding via the saddle point  $TS_{1-2}$ . From a structural point of view,  $TS_{1-2}$  bears already large similarity to **2**. The C–C bond is substantially stretched to 2.049 Å, while the Co–C distance is very close to the bond length found in **2**. The transition vector related to the imaginary frequency of 332i cm<sup>-1</sup> is shown in Figure 1 and clearly indicates the breaking of the C–C bond and the reorientation of the methyl groups. The relative energy of this transition state is 8 kcal mol<sup>-1</sup> below the energy of the separated reactants. As documented in Figure 1, significant agostic (i.e., 3 center-2 electron metal–hydrogen–carbon)<sup>25</sup> interactions between the positively charged metal center and the adjacent hydrogens are present in  $TS_{1-2}$ , which results in typical geometrical distortions, i.e., a close contact between two hydrogens and the cobalt atom (2.079 Å) and elongation of the suitable  $\beta$ -C–H bonds to 1.123 Å and a decrease of the corresponding C–C–H angles.

Proceeding along the reaction coordinate, **2** is converted into **3**, a  $C_{2v}$  symmetric complex between methane and  $CoCH_2^+$ , which serves as the direct precursor for the loss of methane. The methane moiety in **3** is  $\eta^2$  coordinated to the cobalt with a metal carbon distance of 2.345 Å. Apart from the elongated C–Co bond, this is qualitatively the same picture as discussed in great detail by Perry *et al.*<sup>23</sup> (these authors found a value of 2.24 Å for the Co–C bond distance) for the isolated complex  $Co(CH_4)^+$ . The geometry of the cobalt–carbene unit is only slightly distorted from that of the free  $CoCH_2^+$  and has a typical Co–C distance of 1.835 Å. An  $\eta^3$  coordinated complex has also been located ca. 1 kcal mol<sup>-1</sup> less stable than **3** but was identified as a saddle point with an imaginary frequency of 142i cm<sup>-1</sup>. Species **3** is computed to be 5 kcal mol<sup>-1</sup> below the energy of the separated reactants.

**2** and **3** are connected through a direct, one-step 1,3-H migration occurring via saddle point  $TS_{2-3}$ . The transition vector connected to the imaginary frequency of 1435i cm<sup>-1</sup> (shown in Figure 2) and the geometry of this transition structure are completely consistent with the notion of a 1,3-H shift, directly leading to the formation of a methane complex. The concerted nature of  $TS_{2-3}$  contrasts the suggested mechanistic scenario of Armentrout and Beauchamp, who proposed a stepwise reaction profile for the reductive elimination of methane, in which a C–H inserted species  $H(CH_3)Co^+=CH_2$  is involved as a stable intermediate.<sup>26</sup> All our attempts to locate such an inserted minimum for the  $[Co, C_2, H_6]^+$  system lead instead to **2** or **3**.  $TS_{2-3}$  has one elongated and one shortened C–Co bond, and the carbene structure is already preformed.

(24) The main emphasis in this very interesting work is on the observation of an unphysical breaking of  $C_{2v}$  symmetry if only intermediate levels of electron correlation are employed: Perry, J. K.; Goddard, W. A., III; Ohanessian, G. *J. Chem. Phys.* **1992**, *97*, 7560. Such problems did not occur in the present B3LYP calculations.

(25) (a) Brookhart, M.; Green, M. L. H. *J. Organomet. Chem.* **1983**, *250*, 395. (b) Goddard, R. J.; Hoffmann, R.; Jemmis, E. D. *J. Am. Chem. Soc.* **1980**, *102*, 7667. (c) Grubbs, R. H.; Coates, G. W. *Acc. Chem. Res.* **1996**, *29*, 85.

(26) Armentrout, P. B.; Beauchamp, J. L. *J. Am. Chem. Soc.* **1981**, *103*, 784.

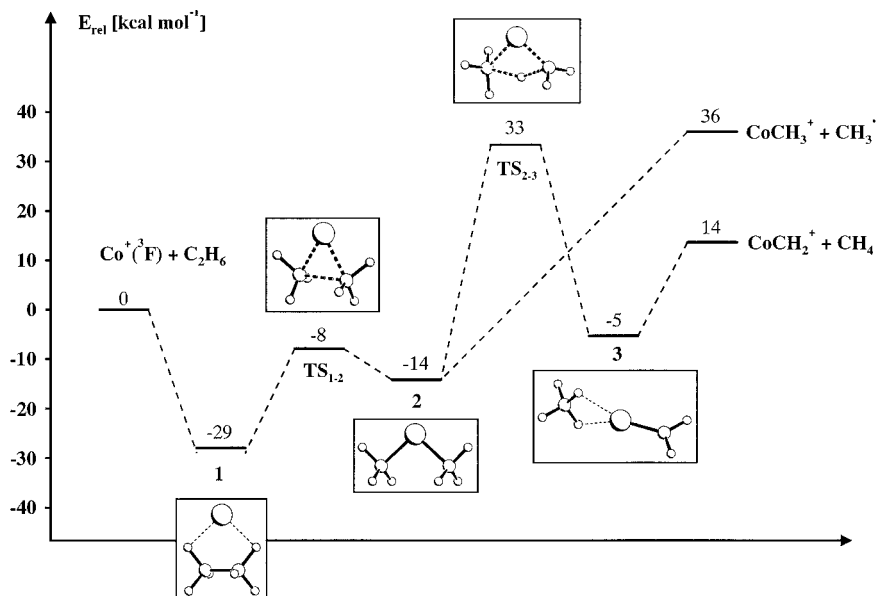


**Figure 2.** C–C bond activation branch of the  $[\text{Co}, \text{C}_2, \text{H}_6]^+$  PES (B3LYP results).

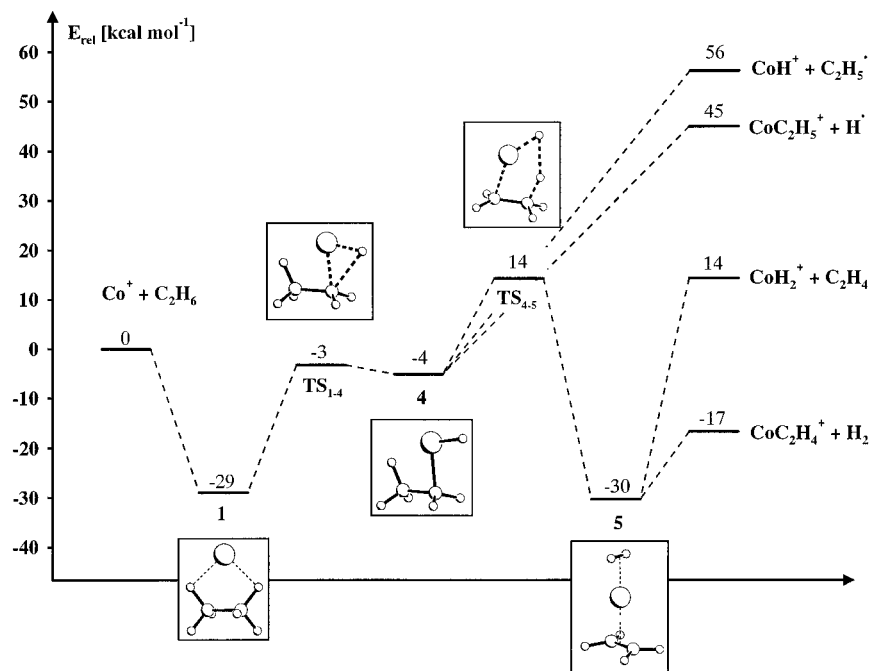


**Figure 3.** C–H bond activation branch of the  $[\text{Co}, \text{C}_2, \text{H}_6]$  PES (B3LYP results).

One important structural feature is the rather short Co–H distance of the migrating hydrogen, which points to a stabilizing interaction between the metal and the migrating hydrogen in the transition structure. With respect to its relative energy,  $\text{TS}_{2-3}$  is by far the most demanding point in the mechanistic scheme for the C–C bond activation, lying 33 and 47 kcal mol<sup>-1</sup> above the isolated reactants and **2**, respectively. The dissociation of **3** into  $\text{CoCH}_2^+$  (<sup>3</sup>A<sub>2</sub>) + CH<sub>4</sub> requires 19 kcal mol<sup>-1</sup>, and the overall reaction  $\text{Co}^+ (^3\text{F}) + \text{C}_2\text{H}_6 \rightarrow \text{CoCH}_2^+ (^3\text{A}_2) + \text{CH}_4$  is endothermic by 14 kcal mol<sup>-1</sup>. The direct fragmentation process cleaving a Co–C bond in the dimethyl species **2** leading to  $\text{CoCH}_3^+ + \text{CH}_3^*$  is only slightly more energetically demanding than  $\text{TS}_{2-3}$ . Due to the entropic bottleneck associated with  $\text{TS}_{2-3}$ , the direct bond cleavage to yield  $\text{CoCH}_3^+$  should be favored in experiments at elevated internal energies on dynamical grounds.

**C–H Bond Activation.** The structures of the stationary points along the C–H bond activation branch of the  $[\text{Co}, \text{C}_2, \text{H}_6]^+$  PES are also collected in Figure 1, while the PES is displayed

in Figure 3. The C–H bond activation pathway branches off the C–C bond activation route after the formation of the initial complex **1**, which is common to both processes. C–H bond activation is initiated by insertion of the  $\text{Co}^+$  into a C–H bond, leading to structure **4**. This species is characterized by a significant agostic interaction between the appropriate C–H bond and the metal centers as indicated by the rather short Co–H distance of only 2.091 Å and the elongation of the corresponding C–H bond to 1.129 Å. Energetically, **4** is 25 kcal mol<sup>-1</sup> above **1** or 4 kcal mol<sup>-1</sup> below the energy of  $\text{Co}^+ (^3\text{F}) + \text{C}_2\text{H}_6$ . The corresponding transition structure  $\text{TS}_{1-4}$  is slightly higher than the C–C insertion saddle point  $\text{TS}_{1-2}$  but is still fairly low in energy, only 1 kcal mol<sup>-1</sup> above **4** (or, equivalently, 3 kcal mol<sup>-1</sup> below the separated reactants). This saddle point occurs very “late” on the reaction coordinate and bears already great similarity to the final structure, **4**. In particular, the agostic interaction discussed above for **4** is already present in  $\text{TS}_{1-4}$ , with the relevant Co–H distance being only 0.071 Å longer than in **4**. The transition vector associated with

the imaginary frequency of  $398i \text{ cm}^{-1}$  confirms  $\text{TS}_{1-4}$  as the correct saddle point for the C–H insertion reaction (Figure 1). In a very recent theoretical paper mainly dealing with the stability and structure of  $\text{H–Co}^+–\text{CH}_3$ , Hendrickx et al.<sup>27</sup> also briefly mention the stability of  $\text{H–Co}^+–\text{C}_2\text{H}_5$ . They use geometries optimized at the complete active space SCF (CASSCF) level and energies obtained at second-order perturbation theory employing a CASSCF reference space (CASPT2). Interestingly, their most favorable geometry of the inserted species differs significantly from that found at B3LYP for **4**: The conformation of the ethyl ligand is staggered with a C–C bond that is eclipsed with respect to the Co–H bond. A *cis* arrangement is found for H–Co–C–C. Thus, no agostic interaction between the metal and a  $\beta$ -CH bond is possible in this conformation. Energetically, they compute relative energies of 18.0 and 24.6 kcal mol<sup>-1</sup> for the equivalents of  $\text{TS}_{1-4}$  and **4**, respectively. Hence, at this level of theory, the saddle point for the C–H bond insertion is above the entrance channel, similar to the result obtained from our CCSD(T) energy calculations (see below). It is interesting to note that the C–H inserted species is actually computed to be even higher in energy than the transition structure, pointing to severe differences between the CASSCF and CASPT2 potential energy surfaces (at CASSCF, the saddle point is of course higher in energy than the associated minima). Thus, from these results, our own CCSD(T) calculations presented below, and the B3LYP data, it cannot be ruled out that  $\text{TS}_{1-4}$  is located actually slightly above the energy of the entrance channel. Proceeding further along the reaction coordinate, the C–H inserted species either can undergo direct bond cleavages leading to  $\text{CoC}_2\text{H}_5^+$  ( $^4A'$ ) + H $\cdot$  or  $\text{CoH}^+$  ( $^4\Phi$ ) +  $\text{C}_2\text{H}_5\cdot$ , computed to be endothermic by 45 and 56 kcal mol<sup>-1</sup> with respect to  $\text{Co}^+$  ( $^3F$ ) +  $\text{C}_2\text{H}_6$ , or can rearrange in a concerted fashion into a rather stable complex **5**, energetically located 30 kcal mol<sup>-1</sup> below the  $\text{Co}^+$  ( $^3F$ ) +  $\text{C}_2\text{H}_6$  asymptote. Just as for the C–C bond activation branch, it is this second step in the reaction mechanism of the C–H bond activation which represents the energetical bottleneck. The saddle point associated with the rearrangement ( $\text{TS}_{4-5}$ ) and its direct connection to both minima has been carefully confirmed by an intrinsic reaction coordinate (IRC)<sup>28</sup> analysis, following the transition vector in both directions. The relative energy of  $\text{TS}_{4-5}$  with respect to the entrance channel amounts to 14 kcal mol<sup>-1</sup> which translates into an activation barrier for the rearrangement as high as 18 and 44 kcal mol<sup>-1</sup> with respect to **4** and **5**, respectively. We note in passing that, in addition to a stepwise mechanism via a dihydrido species, the concerted nature of a reductive H<sub>2</sub> elimination has been assumed previously in an experimental work of van Koppen et al., analyzing the kinetic energy release distribution in the reaction of Fe<sup>+</sup> and propane.<sup>29</sup> In spite of carefully searching, we could not localize a dihydrido species (see discussion below). The equilibrium geometry obtained for the product complex **5** is very similar to the related iron compound. The H<sub>2</sub> unit is perpendicular to the C<sub>2</sub>H<sub>4</sub> moiety (a coplanar arrangement is slightly higher in energy and exhibits an imaginary frequency of  $200i \text{ cm}^{-1}$ ). The distance from the midpoints of the H–H and C–C bonds to the Co center are determined to be 1.742 and 2.028 Å, respectively. The H–H distance in **5** is somewhat elongated as compared to the bond length computed for free H<sub>2</sub> of 0.743 Å. Also the ethylene moiety shows the geometrical

(27) Hendrickx, M.; Ceulemans, M.; Vanquickenborn, L. *Chem. Phys. Lett.* **1996**, *257*, 8.

(28) For details of the IRC approach, see: (a) Gonzales, C.; Schlegel, H. B. *J. Phys. Chem.* **1989**, *90*, 2154. (b) Fukui, K. *J. Phys. Chem.* **1970**, *74*, 4161.

(29) van Koppen, P. A. M.; Bowers, M. T.; Fisher, E. R.; Armentrout, P. B. *J. Am. Chem. Soc.* **1994**, *116*, 3780.

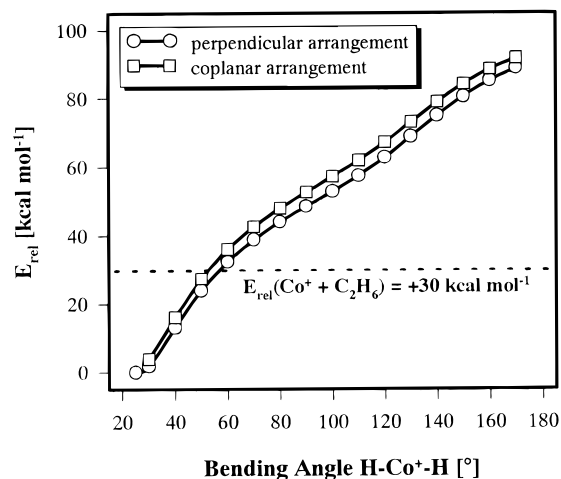


Figure 4. Scan of the H–Co–H angle in **5** (B3LYP results).

distortions expected from the Dewar–Chatt–Duncanson  $\pi(\text{C–C}) \rightarrow 4s(\text{Fe})$  donation and  $3d_{yz}(\text{Fe}) \rightarrow \pi^*(\text{C–C})$  back-donation picture of the bonding interaction: The C–C bond length is 0.05 Å longer than in isolated ethylene, and the CH<sub>2</sub> groups show a small degree of pyramidalization, increasing the overlap of the  $\pi$ -system with the metal orbitals. Once **5** is reached, this complex can break up by expulsion of either molecular hydrogen or ethylene, corresponding to the two exit channels (i)  $\mathbf{5} \rightarrow \text{CoC}_2\text{H}_4^+$  ( $^3A_2$ ) + H<sub>2</sub> or (ii)  $\mathbf{5} \rightarrow \text{CoH}_2^+$  ( $^3A_2$ ) + C<sub>2</sub>H<sub>4</sub>. The threshold for process i is computed as 13 kcal mol<sup>-1</sup> (in other words,  $\text{CoC}_2\text{H}_4^+$  ( $^3A_2$ ) + H<sub>2</sub> is 17 kcal mol<sup>-1</sup> below  $\text{Co}^+$  ( $^3F$ ) + C<sub>2</sub>H<sub>6</sub>), while process ii is much less favorable with a relative energy with respect to **5** of 44 kcal mol<sup>-1</sup> (or 14 kcal mol<sup>-1</sup> above  $\text{Co}^+$  ( $^3F$ ) + C<sub>2</sub>H<sub>6</sub>).

Apart from the fact that this region of the  $[\text{Co}, \text{C}_2, \text{H}_6]^+$  PES is of importance since it represents the decisive region in terms of energy for the reductive H<sub>2</sub> elimination, it is of additional relevance due to the controversial discussion regarding the possible existence of a dihydrido minimum (H<sub>2</sub>)CoC<sub>2</sub>H<sub>4</sub><sup>+</sup>. Such species were frequently suggested as a key intermediate in previous experimental studies on the C–H bond activations by bare transition metal cations.<sup>26,29,30</sup> A scan of the H–Co–H bending angle with all other parameters optimized in both a perpendicular and a coplanar arrangement of the H<sub>2</sub> and the C<sub>2</sub>H<sub>4</sub> moieties in **5** reveals that the region where the inserted  $\text{Co}(\text{H})_2^+$  is expected to occur in some 50 kcal mol<sup>-1</sup> higher in energy as compared to the noninserted species (Figure 4). This is in harmony with reports by Bauschlicher et al.<sup>31</sup> and Perry et al.,<sup>23</sup> who find an electrostatically bound complex between  $\text{Co}^+$  ( $^3F$ ) and molecular hydrogen, but no stable dihydride,  $\text{Co}(\text{H})_2^+$ , in which  $\text{Co}^+$  has inserted into the H<sub>2</sub> bond. Furthermore, in their elaborate CASSCF/MRCI study on the reactions of  $\text{CoCH}_2^+ + \text{H}_2$ , Musaev et al. reported a mechanistic picture of this reaction sequence which bears large similarities to the present discussion.<sup>32</sup> These authors explicitly exclude the existence of a dihydrido species (H<sub>2</sub>)Co=CH<sub>2</sub> along the  $\text{CoCH}_2^+ + \text{H}_2 \rightarrow \text{CoCH}_4^+$  reaction coordinate. Rather, their study reveals a concerted, four-centered transition structure as rate limiting.<sup>32</sup> Thus, the present results confirm our earlier state-

(30) (a) Carpenter, C. J.; van Koppen, P. A. M.; Bowers, M. T. *J. Am. Chem. Soc.* **1995**, *117*, 10976. (b) van Koppen, P. A. M.; Brobelt-Lustig, J.; Bowers, M. T.; Dearden, D. V.; Beauchamp, J. L.; Fisher, E. R.; Armentrout, P. B. *J. Am. Chem. Soc.* **1991**, *113*, 2359.

(31) Bauschlicher, C. W., Jr.; Partridge, H.; Langhoff, S. R. *J. Phys. Chem.* **1992**, *96*, 2475.

(32) (a) Musaev, D. G.; Morokuma, K. *Isr. J. Chem.* **1993**, *33*, 307; (b) Musaev, D. G.; Morokuma, K.; Koga, N.; Nguyen, K. A.; Gordon, M. S.; Cundari, T. R. *J. Phys. Chem.* **1993**, *97*, 11435.

ment<sup>4</sup> that the dihydrido species does not represent a key intermediate in the C–H bond activation, neither for the [Fe,C<sub>2</sub>H<sub>6</sub>]<sup>+</sup> nor for the [Co,C<sub>2</sub>H<sub>6</sub>]<sup>+</sup> system.<sup>33,34</sup> From a qualitative point of view, the thermochemistry of the H–H insertion process in **5** is caused by the balance between several stabilizing and destabilizing contributions: (i) Given  $D_0(\text{H–H}) = 104 \text{ kcal mol}^{-1}$  and  $D_0(\text{Co}^+\text{–H}) = 46 \text{ kcal mol}^{-1}$  and assuming bond additivity for the experimentally unknown second Co–H bond dissociation energy, the insertion is an endothermic process. (ii) The binding of the ethylene ligand in **5** can be understood in terms of the donation/back-donation picture of the Dewar–Chatt–Duncanson model and is moderated by additional population of the 4s orbital at Co<sup>+</sup> due to the presence of either donating ligands or covalent bonds to the cobalt atom. The formation of two covalent bonds to the Co<sup>+</sup> atom involves binding to the 4s orbital at the cobalt atom to a certain amount. The additional 4s electron density reduces the stabilizing  $\pi \rightarrow 4s$  donation from ethylene to Co<sup>+</sup>. Correspondingly we found in our calculations, e.g. in the perpendicular arrangement of H<sub>2</sub> and C<sub>2</sub>H<sub>4</sub>, that the Co–ethylene distance is elongated from 2.028 to 2.196 Å upon bending the H–Co–H angle in **5** from 25° in the minimum to 90°, the region where a hypothetical cobalt–dihydrido complex is expected. The 4s electron population increases from 0.24 in **5** to 0.6 in the 90° structure, according to an NBO population analysis.<sup>35</sup> (iii) Following ideas put forward by Carter and Goddard<sup>36</sup> and Mandich et al.,<sup>37</sup> the formation of covalent bonds

(33) These results, i.e., that a dihydrido minimum does not exist and that the rate-limiting steps are not the primary insertions but the subsequent concerted rearrangement reactions have most probably far-reaching consequences for the interpretation of recent gas phase experiments on the transition metal ion mediated C–H bond activation in larger alkanes. In one of the most insightful studies to date, von Koppen et al.<sup>29</sup> combined results from ion beam experiments and the determination of kinetic energy release distributions with an extensive analysis based on phase space theory for the system Co<sup>+</sup>/propane. Their results were interpreted in terms of a rate-determining saddle point associated with the initial insertion of a Co<sup>+</sup> into a C–H bond (corresponding to **TS**<sub>1–4</sub> in the present context). In addition, they proposed the existence of two different reaction mechanisms for the H<sub>2</sub> elimination in the reaction Co<sup>+</sup> + C<sub>3</sub>H<sub>8</sub>. Our calculations on the [Co,C<sub>3</sub>H<sub>8</sub>]<sup>+</sup> PES in fact yield two energetically similar routes for the expulsion of molecular hydrogen, involving  $\alpha$ - and  $\beta$ -CH-inserted species, respectively (while we identified, of course, only one such reaction pathway for the H<sub>2</sub> loss in the present system). However, just as for the presently discussed Co<sup>+</sup> + C<sub>2</sub>H<sub>6</sub> PES, the calculations predict the initial insertion reactions as not being rate determining. An in-depth discussion of these results pertinent to the [Co,C<sub>3</sub>H<sub>8</sub>]<sup>+</sup> PES is beyond the scope of the present work and will be published in due course (Holthausen, M. C.; Dargel, T. K.; Koch, W. Manuscript in preparation).

(34) In their recent experimental work, Haynes et al. described the presence of a second high-energy feature in the Co(C<sub>2</sub>H<sub>4</sub>)<sup>+</sup> cross section.<sup>45</sup> With regard to these findings, a reviewer mentioned the potential existence of an alternative mechanism for the elimination of H<sub>2</sub> from Co(C<sub>2</sub>H<sub>6</sub>)<sup>+</sup>. Although we do not have a straightforward explanation for these observations on the basis of our computations so far, we like to rule out an alternative mechanism via dihydrido minima on the triplet potential energy surface. Haynes et al. suggested the formation of Co(C<sub>2</sub>H<sub>4</sub>)<sup>+</sup> + 2H or a reaction of one of the primary product ions, i.e. CoCH<sub>2</sub><sup>+</sup>, with C<sub>2</sub>H<sub>6</sub> to form the Co(C<sub>2</sub>H<sub>4</sub>)<sup>+</sup> product ion as potential reactions. While these reaction pathways are outside the scope of our present contribution, we agree with the reviewer's assumption that, in the high-energy regime, where the second feature occurs (i.e., at about 4 eV elevated energies), excited state potential energy surfaces may get involved. Although the <sup>1</sup>D atomic state is well separated from the <sup>3</sup>F atomic ground state by about 1.4 eV and most probably does not play a role under thermal conditions, curve crossing processes may take place at such elevated energies and may contribute significantly to the kinetic behavior of the system under study. A prerequisite for investigations along these lines would be the availability of algorithms capable of geometry optimizations/energy minimizations at the seam of crossing between ground and excited state PES at the applied level of theory. At present, no such code is available to us and thus we are restricted to the investigation of minimum energy reaction pathways, which occur on a single PES.

(35) Reed, A. E.; Curtiss, L. A.; Weinhold, F. *Chem. Rev.* **1988**, *88*, 899.

(36) Carter, E. A.; Goddard, W. A., III. *J. Phys. Chem.* **1988**, *92*, 5679.

involves promotion of the Co<sup>+</sup> atom to an excited state from which the binding is accomplished and is connected with the loss of exchange energy in the range 10–40 kcal mol<sup>-1</sup> in this case.

It is interesting to note, however, that dihydrido minima do exist for earlier first-row transition metal ions in the gas phase and such species in fact are referred to as “classical” isomers in condensed phase chemistry, whereas complexes with molecular hydrogen are termed “nonclassical”.<sup>38</sup> In a recent study of Bushnell et al. and in two former studies of Rappe and Upton and Alvarado-Swaisgood and Harrison, it was shown<sup>39</sup> that for Sc<sup>+</sup>(H<sub>2</sub>) in fact a second minimum exists in which Sc<sup>+</sup> is inserted into the H<sub>2</sub> bond. While these findings can already be understood in terms of thermochemistry ( $D_0(\text{Sc}^+\text{–H}) = 57 \text{ kcal mol}^{-1}$  and  $D_0(\text{HSc}^+\text{–H}) = 58 \text{ kcal mol}^{-1}$ ), the existence of such species might be decisive in the course of reactions with alkanes. The efficient reactions of Sc<sup>+</sup> with ethane<sup>40</sup> may possibly be attributed to energetically less demanding stepwise reaction mechanisms via dihydrido species.

Another interesting feature of our calculated PES concerns the finding of a higher transition state **TS**<sub>1–4</sub> for the primary C–H insertion as compared to the primary C–C insertion transition state **TS**<sub>1–2</sub>. This contrasts results of Blomberg et al. and Low and Goddard, studying alkane activation processes mediated by neutral transition metal atoms.<sup>41</sup> In all cases, the C–H insertion has been found to be significantly less energy demanding as compared to the initial C–C activation barriers. As discussed in detail by these authors, the higher C–C activation barriers have been attributed to a directionality of the singly occupied sp<sup>3</sup> orbital of methyl groups. While the H(1s) orbital can simultaneously overlap with both the metal center and the methyl group, the bond breaking/formation in the dimethyl case involves a reorientation of the CH<sub>3</sub> moiety, which gives rise to an additional barrier for C–C activation processes. In the context of our present findings, we point out that for cationic systems additional effects become important. For example, there are two significant agostic interactions, with one of the C–H bonds of each methyl groups in **TS**<sub>1–2</sub>, while in the case of **TS**<sub>1–4</sub>, only one such interaction is present (Figure 1). A closer look back to the initial C–C and C–H barriers in the reaction of Fe<sup>+</sup> with ethane<sup>4</sup> reveals, notwithstanding the inherent differences of these two systems, that the optimum geometry of the corresponding structure **TS**<sub>1–2</sub> has only one such interaction, as has the corresponding structure **TS**<sub>1–4</sub> and both activation barriers are of equal height. Another explanation for the supposedly wrong ordering or barrier heights in the cationic cases could be the missing electrostatic stabilization in the transition state for neutral species. This stabilization will be significantly better for a methyl group since it is substantially more polarizable than a hydrogen atom.<sup>42</sup> Perry has pointed out that the close contact of the metal to a negatively charged carbon as compared to a neutral or slightly positively charged

(37) Mandich, M. L.; Halle, L. F.; Beauchamp, J. L. *J. Am. Chem. Soc.* **1984**, *106*, 4403.

(38) See, e.g.: Dedieu, A., Ed. *Transition Metal Hydrides*; VCH: New York, 1992.

(39) (a) Bushnell, J. E.; Kemper, P. R.; Maitre, P.; Bowers, M. T. *J. Am. Chem. Soc.* **1994**, *116*, 9710. (b) Rappe, A. K.; Upton, T. H. *J. Chem. Phys.* **1986**, *85*, 4400. (c) Alvarado-Swaisgood, A. E.; Harrison, J. F. *J. Phys. Chem.* **1985**, *89*, 5198.

(40) See, e.g.: Armentrout, P. B.; Beauchamp, J. L. *Acc. Chem. Res.* **1989**, *22*, 315.

(41) (a) Blomberg, M. R. A.; Siegbahn, P. E. M.; Nagashima, U.; Wennerberg, J. *J. Am. Chem. Soc.* **1991**, *113*, 424. (b) Blomberg, M. R. A.; Brandemark, U.; Siegbahn, P. E. M. *Ibid.* **1983**, *105*, 5557. (c) Low, J. J.; Goddard, W. A., III. *Ibid.* **1984**, *106*, 8321. (d) Low, J. J.; Goddard, W. A., III. *Ibid.* **1986**, *108*, 6115. (e) Low, J. J.; Goddard, W. A., III. *Organometallics* **1986**, *5*, 609.

**Table 3.** ZPVE Corrected Energy Differences from B3LYP and CCSD(T) Calculations Relative to the  $\text{Co}(\text{CH}_3)_2$  Species **2** in kcal  $\text{mol}^{-1}$ 

species	B3LYP	CCSD(T) <sup>a</sup>
<b>1</b>	–15	–22
<b>3</b>	9	6
<b>4</b>	10	10
<b>5</b>	–16	–19
<b>TS</b> <sub>1–2</sub>	6	4
<b>TS</b> <sub>2–3</sub>	47	48
<b>TS</b> <sub>1–4</sub>	11	12
<b>TS</b> <sub>4–5</sub>	28	27
$\text{Co}^+(\text{F}) + \text{C}_2\text{H}_6$	14	–2
$\text{CoCH}_3^+ + \text{CH}_3^\bullet$	50	42
$\text{CoCH}_2^+ + \text{CH}_4$	28	25
$\text{Co}(\text{H}_2)^+ + \text{C}_2\text{H}_4$	28	20
$\text{Co}(\text{C}_2\text{H}_4)^+ + \text{H}_2$	–3	–8
$\text{CoH}^+ + \text{C}_2\text{H}_5^\bullet$	70	57
$\text{CoC}_2\text{H}_5^+ + \text{H}^\bullet$	59	51

<sup>a</sup> Using the optimized geometries and ZPVE contributions from the B3LYP calculations.

hydrogen neighbor should have an effect in the same direction.<sup>43</sup> Part of the lower energy demand of the primary C–C insertion process versus C–H bond activation is certainly due to the underestimation of the  $\text{H}_3\text{C}–\text{CH}_3$  BDE (cf. Table 1), but even if one assumes that the different errors for the C–C and C–H BDE are completely transferred to the saddle point energies, the C–C insertion barrier (**TS**<sub>1–2</sub>) will be of comparable energy to the C–H insertion (**TS**<sub>1–4</sub>) but certainly not significantly above it. It appears to be a general feature that the relative barrier heights of neutral and cationic systems differ in nature due to the additional presence of stabilizing effects in case of charged species.

In order to validate our results and in particular the relative barrier heights in the current system further, we performed a series of CCSD(T) energy calculations on the B3LYP geometries for all critical points and the fragmentation channels on the  $[\text{Co}, \text{C}_2, \text{H}_6]^+$  PES. Table 3 demonstrates an excellent agreement in the relative energies of the minima and saddle points. The relative energetic ordering of the minima obtained at the CCSD(T) level as well as the barrier heights are in complete agreement with the B3LYP results. The largest deviation occurs for **1** which at the CCSD(T) level is predicted to be 22 kcal  $\text{mol}^{-1}$  lower than **2**, while at B3LYP, an energy difference of only 15 kcal  $\text{mol}^{-1}$  is obtained. For all other relative energies the two sets of data differ by no more than 3 kcal  $\text{mol}^{-1}$ . Particularly satisfying is the almost quantitative agreement in the relative heights of the transition structures. Much larger deviations are observed for the relative energies of the entrance and exit channels. Here, CCSD(T) consistently yields lower relative energies by up to 13 kcal  $\text{mol}^{-1}$  than B3LYP. A comparison of the computed binding energy of **1** (20 kcal  $\text{mol}^{-1}$  with respect to separated  $\text{Co}^+ + \text{C}_2\text{H}_6$ ) to the probably best experimental number available ( $28.0 \pm 1.6$  kcal  $\text{mol}^{-1}$ <sup>18</sup>) clearly indicates problems of the applied *post*-HF approach in a balanced description of correlation energy contributions for bond dissociation processes. On the other hand, the description of relative energies of similarly bound species is apparently less problematic; obviously, a similar amount of correlation energy is present in any of these structures and shortcomings of the chosen CCSD(T) approach cancel out. It is, however, well-known that a reliable determination of

(42) The same argument has been proposed as an explanation for the observation that  $D_0(\text{Co}^+–\text{CH}_3) > D_0(\text{Co}^+–\text{H})$  by 9 kcal  $\text{mol}^{-1}$ . See, e.g.: Armentrout, P. B. In *Selective Hydrocarbon Activation*; Davies, J. A.; Watson, P. L.; Liebman, J. F.; Greenberg, A., Eds.; VCH: New York: 1990.

(43) Perry, J. K. Personal communication.

metal–ligand binding energies at the CCSD(T) (or any other conventional correlated method) requires much larger and more flexible basis sets than the one used here,<sup>44</sup> and therefore, these results should be taken with great caution. Overall, the CCSD(T) calculations lead to the same qualitative picture of the bond activation processes in the  $[\text{Co}, \text{C}_2, \text{H}_6]^+$  system. In particular, the central conclusions drawn above, such as (i) the significantly larger barriers associated with the multicenter saddle points **TS**<sub>2–3</sub> and **TS**<sub>4–5</sub> as compared to the activation energies of the initial C–C and C–H insertion processes and (ii) the lower activation energy for the C–C insertion (**TS**<sub>1–2</sub>) as compared to the C–H insertion (**TS**<sub>1–4</sub>), are fully confirmed at the CCSD(T) level of theory. To the best of our knowledge, this is the first validation of B3LYP results for barrier heights on open-shell metal organic systems, and the encouraging results corroborate the internal consistency of the chosen B3LYP approach.

**Comparison with Recent Gas Phase Experiments.** In this section, we will briefly compare our theoretical findings with results from a very recent experimental study by Haynes et al.<sup>45</sup> In this investigation several bimolecular reactions, i.e.  $\text{Co}^+ + \text{C}_2\text{H}_6$ ,  $\text{Co}(\text{C}_2\text{H}_4)^+ + \text{H}_2$  ( $\text{D}_2$ ), and  $\text{Co}=\text{CH}_2^+ + \text{CH}_4$  ( $\text{CD}_4$ ) as well as threshold collisional activation of  $\text{Co}(\text{C}_2\text{H}_6)^+$  with Xe have been used in order to probe different regions on the  $[\text{Co}, \text{C}_2, \text{H}_6]^+$  PES. Now, much more detailed thermodynamic information on intermediates and transition barriers is available than from previous experimental studies on this system.<sup>26,46</sup> In the reaction of  $\text{Co}^+$  with ethane, two major product channels are observed, leading to  $\text{Co}–\text{H}^+$  and  $\text{Co}–\text{CH}_3^+$ , respectively. The measured energy thresholds for two endothermic reactions ( $\text{Co}^+ + \text{C}_2\text{H}_6 \rightarrow \text{CoCH}_3^+ + \text{CH}_3^\bullet$ ,  $39.4 \pm 0.9$  kcal  $\text{mol}^{-1}$ ;  $\text{Co}^+ + \text{C}_2\text{H}_6 \rightarrow \text{CoH}^+ + \text{C}_2\text{H}_5^\bullet$ ,  $53.7 \pm 1.4$  kcal  $\text{mol}^{-1}$ ) compare well with our calculated  $D_0$  values of 36 and 56 kcal  $\text{mol}^{-1}$ , respectively. However, there seems to be an inconsistency between these observations and the fact that we compute a lower endothermicity for the process **4**  $\rightarrow$   $\text{CoC}_2\text{H}_5^+ + \text{H}^\bullet$  (which is *not* observed experimentally) than for the loss of an ethyl radical, which is also generated from **4** via direct bond cleavage. This lower energy demand for the loss of a hydrogen atom is found not only at B3LYP but, albeit to a less extent, also in our CCSD(T) calculations (see Table 3). Furthermore, even if the experimental data are used, a slight preference of 1 kcal  $\text{mol}^{-1}$  for this process as compared to the expulsion of an ethyl radical remains (Table 1). Thus it seems that, while B3LYP apparently exaggerates the energy difference between these two fragmentation channels, it is nevertheless the energetically less favored one which is actually observed experimentally. Such a behavior is, however, not without precedents and is rationalized in terms of angular momentum arguments as alluded to by Haynes et al.<sup>45</sup> and explained in detail by Aristov and Armentrout for the case of the reaction between  $\text{V}^+ + \text{CH}_4$ , where the most efficient reaction leads to  $\text{VH}^+ + \text{CH}_3^\bullet$ , even though the fragmentation according to  $\text{V}^+ + \text{CH}_4 \rightarrow \text{VCH}_3^+ + \text{H}^\bullet$  is favored energetically by some 0.1 eV.<sup>47</sup> The elimination of molecular  $\text{H}_2$  from ethane is the only exothermic reaction channel observed and has the lowest threshold among all

(44) See, e.g.: Bauschlicher, C. W., Jr.; Langhoff, S. R.; Partridge, H. In *Modern Electronic Structure Theory*; Yarkony, D. R., Ed.; World Scientific: Singapore, 1995.

(45) Haynes, C. L.; Fisher, E. R.; Armentrout, P. B. *J. Am. Chem. Soc.* Submitted for publication.

(46) Georgiadis, R.; Fisher, E. R.; Armentrout, P. B. *J. Am. Chem. Soc.* **1989**, *111*, 4251.

(47) Aristov, N.; Armentrout, P. B. *J. Phys. Chem.* **1987**, *91*, 6178.

(48) Bauschlicher, C. W., Jr.; Partridge, H.; Sheehy, J. A.; Langhoff, S. R.; Rosi, M. *J. Phys. Chem.* **1992**, *96*, 6969.

(49) Petterson, L. G. M.; Bauschlicher, C. W., Jr.; Langhoff, S. R. *J. Chem. Phys.* **1987**, *87*, 481.



products. The measured barrier height is  $7.4 \pm 2.8$  kcal mol<sup>-1</sup> with respect to the separated  $\text{Co}^+ + \text{C}_2\text{H}_6$ , in good agreement with our calculated relative energy  $\text{TS}_{4-5}$  of 14 kcal mol<sup>-1</sup>. For the methane elimination process,  $\text{Co}^+ + \text{C}_2\text{H}_6 \rightarrow \text{CO}=\text{CH}_2^+ + \text{CH}_4$ , a barrier height of  $8.3 \pm 5.3$  kcal mol<sup>-1</sup> with regard to the height of the exit channel  $\text{Co}=\text{CH}_2 + \text{CH}_4$  has been measured. From the investigation of the reverse reaction,  $\text{Co}=\text{CH}_2^+ + \text{CH}_4 \rightarrow \text{Co}^+ + \text{C}_2\text{H}_6$ , a barrier height of  $6.4 \pm 2.1$  kcal mol<sup>-1</sup> is obtained. On the basis of these two values, the authors estimated a barrier of  $6.7 \pm 2.1$  kcal mol<sup>-1</sup> with regard to the endothermicity of the exit channel. Our calculated value of 19 kcal mol<sup>-1</sup> is significantly larger, revealing difficulties for the B3LYP functional in the description of the related exit channel (cf. Table 2). If we compare the experimentally determined barriers for the dehydrogenation reaction ( $7.4 \pm 2.8$  kcal mol<sup>-1</sup>) and for the demethanation reaction ( $24.0 \pm 2.5$  kcal mol<sup>-1</sup>) relative to the separated  $\text{Co}^+ + \text{C}_2\text{H}_6$ , the latter is higher in energy by 17 kcal mol<sup>-1</sup>. Our computed difference of 19 kcal mol<sup>-1</sup> now is in much better agreement with the experimental result, again indicating a much better performance of the B3LYP functional for the description of relative energies between similarly bound species as found for the description of different binding situations.

## Conclusion

The following conclusions can be drawn from our quantum chemical investigation on the potential energy surface relevant for the interaction of  $\text{Co}^+$  with ethane:

(i) The only exothermic reaction starting from  $\text{Co}^+$  (<sup>3</sup>F) +  $\text{C}_2\text{H}_6$  corresponds to the formation of  $\text{CoC}_2\text{H}_4^+$  (<sup>3</sup>A<sub>2</sub>) +  $\text{H}_2$ . All other exit channels from the  $[\text{Co}, \text{C}_2, \text{H}_6]^+$  PES are endothermic by at least 14 kcal mol<sup>-1</sup>. Both the C–C and the C–H bond activation branches of the  $[\text{Co}, \text{C}_2, \text{H}_6]^+$  PES are characterized by substantial activation barriers, amounting to 33 and 14 kcal mol<sup>-1</sup>, respectively, compared to the separated reactants. These findings are in complete qualitative agreement with very recent experimental work, although some quantitative deviations occur with respect to the height of the barriers, which seem to be overestimated by the applied DFT/HF model, and a high-energy feature of the  $\text{Co}(\text{C}_2\text{H}_4)^+$  cross section cannot be explained on the basis of our present calculations.<sup>34</sup>

(50) (a) Schilling, J. B.; Goddard, W. A., III; Beauchamp, J. L. *J. Am. Chem. Soc.* **1986**, *108*, 582; (b) Schilling, J. B.; Goddard, W. A., III; Beauchamp, J. L. *J. Phys. Chem.* **1987**, *91*, 5616.

(51) Anglada, J.; Bruna, P. J.; Grein, F. *J. Chem. Phys.* **1990**, *92*, 6732.

(52) Bauschlicher, C. W., Jr.; Langhoff, S. R.; Partridge, H.; Barnes, L. A. *J. Chem. Phys.* **1989**, *91*, 2399.

(53) Maitre, P.; Bauschlicher, C. W., Jr. *J. Phys. Chem.* **1993**, *97*, 11912.

(54) Bauschlicher, C. W., Jr.; Maitre, P. *J. Phys. Chem.* **1995**, *99*, 3444.

(55) Sodupe, M.; Bauschlicher, C. W., Jr.; Langhoff, S. R.; Partridge, H. *J. Phys. Chem.* **1992**, *96*, 2118.

(56) Lias, S. G.; Bartmess, J. E.; Liebman, J. F.; Holmes, J. L.; Levin, R. D.; Mallard, W. G. *J. Phys. Ref. Data, Suppl.* **1988**, *17*, 1.

(ii) The saddle points for insertion of  $\text{Co}^+$  into a C–C or C–H bond ( $\text{TS}_{1-2}$  and  $\text{TS}_{1-4}$ , respectively) are without doubt considerably less energetically demanding than the activation barriers connected with the subsequent steps, i.e., the concerted rearrangement into complexes between methane and  $\text{CoCH}_2^+$  ( $\text{TS}_{2-3}$ , C–C bond activation) and between  $\text{Co}^+$ , molecular hydrogen and ethylene ( $\text{TS}_{4-5}$  C–H bond activation). This order of activation energies is strongly supported by the fact that the relative barrier heights computed at the B3LYP and CCSD(T) levels of theory show almost quantitative agreement with each other.

(iii) The first saddle points along the reaction coordinates of the C–C and C–H bond activation processes, i.e.,  $\text{TS}_{1-2}$  and  $\text{TS}_{1-4}$  are energetically located close to but somewhat lower than the separated reactants. However, on the basis of the present computations, we cannot strictly rule out that their true relative energy is actually slightly above the energy of the entrance channel. For the same reason, it might also be that  $\text{TS}_{1-4}$ , which is computed to be only 1 kcal mol<sup>-1</sup> above **4**, will disappear at more sophisticated levels of theory or upon inclusion of thermal corrections such that also **4** may not represent an intermediate anymore but only a distortion on the reaction coordinate connecting **1** and **5**.

(iv) Overall, in the  $[\text{Co}, \text{C}_2, \text{H}_6]^+$  system, the C–C bond activation is kinetically as well as thermodynamically disfavored compared to the C–H bond activation.

(v) As demonstrated by the comparison to experimental data and the CCSD(T) results, the B3LYP ansatz is capable of accurately describing relative energies between several species in the potential energy surface, which are similarly bound. However, major, nonuniform deviations between calculated and experimental data have been found, if noncovalently bound species are studied. Nonetheless, if used with care, the chosen computational strategy provides a promising compromise between accuracy and computational efficiency and seems to constitute a powerful tool with predictive capabilities for the elucidation of mechanistic details of open-shell transition metal involving reactions.

**Acknowledgment.** We gratefully acknowledge inspiring discussions with Dr. Detlef Schröder, Dr. Andreas Fiedler, Dr. Petra von Koppen, and Dr. Jason Perry. We thank Prof. P. B. Armentrout for a preprint of ref 45. A generous amount of computer time and excellent service (Dr. T. Steinke) was provided by the Konrad-Zuse Zentrum für Informationstechnik. M.C.H. thanks Prof. Helmut Schwarz for financial support. This work was supported by the Deutsche Forschungsgemeinschaft. Finally, we thank the reviewers for helpful suggestions.

JA954090X